Copyright © 2010 Tech Science Press CMES, vol.67, no.2, pp.79-94, 2010

Computational Quantum Mechanics Simulation on the Photonic Properties of Group-III Nitride Clusters

Che-Wun Hong[1,2] **and Chia-Yun Tsai**[1]

Abstract: This paper describes the quantum mechanical simulation on the photonic properties of group-III nitride clusters, whose bulk types are common materials for light emitting diodes (LEDs). In order to emit different colors of light using the same semiconductor materials, it is possible to vary the band gap by controlling the quantum dot sizes or doping a third atom theoretically. Density functional theory (DFT) calculations are performed to analyze a set of binary $(\mathrm{GaN})_n$ ($3 \leq n \leq 32$) and ternary $\mathrm{In}_x\mathrm{Ga}_{1-x}\mathrm{N}$ ($0 \leq x \leq 0.375$) clusters to study their photonic characteristics. The ground state structures are optimized to calculate the binding energies using the time-independent DFT. Then the corresponding density of states (DOS), band gaps, and absorption/excitation energies are evaluated from the time dependent DFT technique. Photoluminescence characteristics are predicted and their relationships with the cluster size and cluster surface effects are studied.

Keywords: light emitting diodes (LEDs), density functional theory (DFT), band gap

1 Introduction

Group-III nitrides are common materials for the modern photo-electric industry, since the first GaN LED was invented in 1960s and later remarkably improved by Nakamura to make mass production possible in 1993 (Nakamura, Fasol, Pearton, 2000). Nakamura developed the first group-III nitride-based blue/green LED, which can be converted to yellow light by phosphor coating, is the key technology to white LED lighting (Nakamura, Mukai, Senoh, 1991; Nakamura, Mukai, 1992; Nakamura, Mukai, Senoh, 1994; Nakamura, Senoh, Iwasa, Nagahama, 1995; Nakamura, Senoh, Nagahama, Iwasa, Yamada, Matsushita, Kiyoku, Sugimoto, Kozaki,

---

[1] Department of Power Mechanical Engineering, National Tsing Hua University, Hsinchu 30013, Taiwan

[2] Corresponding author. Phone: +886-3-5742591; Fax: +886-3-5722840; E-mail: cwhong@pme.nthu.edu.tw

Umemoto, Sano, 1998). The achievement has resulted in significant development in various devices, such as the solid state lighting, displays, and the next generation optical storage. Although the physical and chemical properties of group-III nitrides in their bulk types have been extensively studied both experimentally and theoretically, the photonic characteristics in the quantum dot scale are still under investigation (Zheludev, 2007). Kandalam et al (2002) reported the results of a theoretical study of Al_nN_n, Ga_nN_n and In_nN_n (with n=4, 5, 6) clusters, focusing on their structure properties, stability, and electronic structure. Several researchers also published some reports on the geometric and electronic structures of the group III nitrides (Song, Cao, 2004; Wu, Zhang, Xu, Zhang, Jiao, 2003; Zhao, Wang, Zhou, Chen, Lu, 2006). Quantum confinement effects in gallium nitride nanostructures were studied by Carter et al (2009) using *ab inito* techniques. Surface effects plus the quantum confinement of nano-sized GaN clusters have also been investigated by Brena and Ojamae (2008).

Binary GaN and ternary $In_xGa_{1-x}N$ clusters are the focus of this paper and our research group intends to initiate a theoretical study from nano-scale using the framework of the computational quantum mechanics. Firstly, we built up the hexagonal wurtzite molecular models which included binary $(GaN)_n$ ($3\leq n\leq 32$) and ternary $In_xGa_{1-x}N$ ($0\leq x\leq 0.375$) clusters. Then, we optimized the ground state structures to calculate the binding energies based on the time independent density functional theory (TI-DFT). The corresponding density of states (DOSs), band gaps, and absorption/excitation energies were evaluated from the time dependent density functional theory (TD-DFT). Photoluminescence characteristics of the quantum-dot-like clusters are predicted and the cluster size and surface effects are studied.

First principles calculations were carried out at the platform of a Gaussian09 (Frisch et al, 2009) software by employing the hybrid exchange-correlation functional B3LYP (Becke three-parameter Lee-Yang-Parr) and the LanL2DZ (Los Alamos National Laboratory 2-Double Zeta) basis set. Until now, there are few corresponding research papers published, especially there is none about the absorption and emission properties of III-N quantum dots (QDs) whose diameters are below 2.4nm. It is hoped that this article is able to set up a fundamental design tool and to further improve the future LED performance via the concept of the nanotechnology.

2 Computational Quantum Mechanics

First-principles computational quantum mechanics (Srivastava, Atluri, 2002; Fitzgerald, Goldbeck-Wood, Kung, Petersen, Subramanian, Wescott, 2008) include two fundamental methods: one is called the *ab inito* molecular orbital approach which uses the Hartree-Fock method with the full description of the Slater determinant

(Slater, 1951); the other one is the density functional theory (DFT) approach, which calculates the density functional to evaluate the electronic structure of atoms and molecules in a general poly-electronic system. Instead of mission impossible to calculate the full N-electron wave functions via the *ab inito* approach, the methodology of the DFT only attempts to calculate the total electronic energy and the overall electronic density distribution. The central idea of the DFT is that there is a relationship between the total electronic energy and the overall electronic density. A functional enables a function to be mapped to a number and is usually expressed by square brackets as below:

$$E\left[f(\vec{r})\right] = \int f(\vec{r})dr \tag{1}$$

where $\vec{r}$ is the position vector, the function $f(\vec{r})$ is usually dependent on other well-defined functions. In the DFT, the function $f(\vec{r})$ is the density function $\rho(\vec{r})$, and the energy functional E is a summation of two terms:

$$E\left[\rho(\vec{r})\right] = \int V_{ext}(\vec{r})\rho(\vec{r})dr + F\left[\rho(\vec{r})\right]. \tag{2}$$

The first term at the right hand side represents the interaction of the electrons with an external potential $V_{ext}(\vec{r})$. The second term $F[\rho(\vec{r})]$ is the sum of the kinetic energy of the electrons and the contribution from inter-electronic interactions. A variational approach (Mura, Koya, 1992) can be used to find out the minimum energy functional which corresponds to the exact ground-state electron density. That means a guessed density input will result in an energy value greater than the true energy. We introduce a Lagrange multiplier (-μ) to find out the minimum at

$$\frac{\delta}{\delta\rho(\vec{r})}\left[E\left[\rho(\vec{r})\right] - \mu\int\rho(\vec{r})dr\right] = 0. \tag{3}$$

which leads to

$$\mu = \left(\frac{\delta E\left[\rho(\vec{r})\right]}{\delta\rho(\vec{r})}\right)_{V_{ext}} \tag{4}$$

where the subscript V_{ext} indicates that it is under conditions of constant external potential. The above equation is the DFT equivalent of the Schrödinger equation. Following the work of Kohn and Sham (1965), the approximate functional E is partitioned into several terms:

$$E[\rho(\vec{r})] = E_T[\rho(\vec{r})] + E_V[\rho(\vec{r})] + E_J[\rho(\vec{r})] + E_{XC}[\rho(\vec{r})] \tag{5}$$

where E_T is the kinetic energy term arisen from the motion of the electrons; E_V includes terms describing the potential energy of the nuclear-electron attraction and the repulsion between pairs of nuclei; E_J is the electron-electron repulsion term; and E_{XC} represents the exchange-correlation term which includes the remaining part of the electron-electron interactions. All terms are functionals of the electron density function $\rho(r)$, except the nuclear-nuclear repulsion. Pure DFT methods are defined by pairing an exchange functional with a correlation functional. In this simulation, we adopted the well-known B3LYP (Foresman, Frisch, 1996), which pairs the Becke's gradient-corrected exchange functional with the gradient-corrected correlation functional of Lee, Yang and Parr (1988). This hybrid exchange-correlation functional is constructed as a linear combination of the Hartree-Fock exact exchange functional (E_X^{HF}) and a number of exchange and correlation explicit density functionals, which are expressed by:

$$E_{XC}^{B3LYP} = E_{XC}^{LDA} + a_0(E_X^{HF} - E_X^{LDA}) + a_x(E_X^{GGA} - E_X^{LDA}) + a_c(E_C^{GGA} - E_C^{LDA}) \tag{6}$$

where $a_0 = 0.20$, $a_x = 0.72$, and $a_c = 0.81$are three weighting coefficients, E_X^{GGA} and $E_C^{GGA}$are generalized gradient approximations (GGA) of the Becke exchange functional (Becke, 1988), and the correlation functional of Lee, Yang and Parr (Lee, Yang, Parr, 1988), and E_C^{LDA} is the VWN (Vosko, Wilk, Nusair, 1980) local-density approximation (LDA) to the correlation functional.

The next approximation involves expressing the molecular orbitals as linear combinations of a pre-defined set of single-electron functions known as basis functions. These basis functions are usually centered on the atomic nuclei and so bear some resemblance to atomic orbitals. The Gaussian09 program uses Gaussian-type atomic functions as basis functions, which have the general form as:

$$g(\alpha,\vec{r}) = cx^n y^m z^l \exp(-\alpha r^2) \tag{7}$$

where the vector $\vec{r}$ is composed of the positions of x, y and z; α is a constant determining the size (radial extent) of the function; n, m and l are principal, magnetic and azimuthal quantum numbers, respectively; and c depends on α, n, m and l. In our simulation, we chose the LanL2DZ basis set since all those three atoms, Ga, N and In, involved in this research are within its data base.

The equations described above are for the special case of time-independent density functional theory (TI-DFT). In the more general case, time is dependent, and the Schrödinger equation becomes:

$$i\hbar\frac{\partial\Psi(\vec{r},t)}{\partial t} = \hat{H}[\rho(\vec{r},t)]\Psi(\vec{r},t) \tag{8}$$

$$\hat{H}[\rho(\vec{r},t)] = E_T[\rho(\vec{r},t)] + E_V[\rho(\vec{r},t)] + E_J[\rho(\vec{r},t)] + E_{XC}[\rho(\vec{r},t)] \tag{9}$$

where $\hbar$ is the Planck's constant divided by 2π and i is the square root of -1; $\hat{H}$ is the Hamiltonian operator;Ψ is the wavefunction which characterizes the particle's motion. Note that all the variables are functions of $\vec{r}$ and t, so it is called time-dependent DFT (TD-DFT). The most useful application of the TD-DFT in this paper is in the calculation of the energies of excited states of an isolated system. Such calculations are based on the fact that the linear response function has poles at the exact excitation energies of the system (Runge, Gross, 1984; Marques, Ullrich, Nogueira, Rubio, Burke, Gross, 2006). The linear response function describes how the electron density changes when the external potential varies.

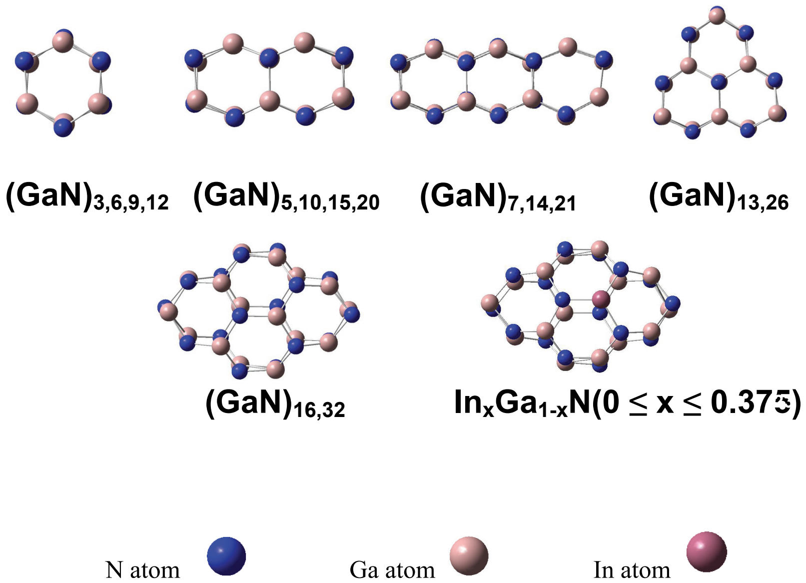

Figure 1: Top views of the molecular structures of the binary $(GaN)_n$ ($3 \leq n \leq 32$) and the ternary $In_xGa_{1-x}N$ ($0 \leq x \leq 0.375$) clusters. Each cluster is composed by a number of rings (varying from 1 to 4) and layers (varying from 1 to 4). Ga atoms are in light purple, N atoms are in blue, and In atoms are in deep purple.

3 Simulation Results and Discussion

Most III-V compounds crystallize in the zincblende lattice structure which belongs to the tetrahedral phases (Madelung, 1964); however, GaN and GaInN semiconductors are in the wurtzite structures (Sze, Ng, 2007). In this paper, we set up the molecular structure of the binary $(GaN)_n$ ($3 \leq n \leq 32$) and the ternary $In_xGa_{1-x}N$ ($0 \leq x \leq 0.375$) clusters to study their photonic characteristics. Figure 1 shows the top views of the molecular structures of the binary $(GaN)_n$ ($3 \leq n \leq 32$) and the ternary $In_xGa_{1-x}N$ ($0 \leq x \leq 0.375$) clusters. Each cluster is composed by a number of rings (varying from 1 to 4) and several layers (varying from 1 to 4). Using the DFT technique, we can optimize those molecular structures at the ground state. That enables us to calculate the binding energy (E_b) of each molecular cluster using the equation as below:

$$E_b \text{ [per GaN unit]} = E[(GaN)_n]/n - E[\text{GaN monomer}] \quad (10)$$

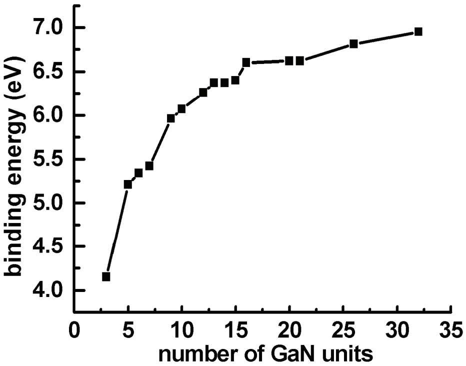

Figure 2: Binding energies of the binary $(GaN)_n$ ($3 \leq n \leq 32$) clusters. The trend indicates that the larger the cluster, the greater the binding energy and hence the more stable structure.

Figure 2 shows the binding energies of the binary $(GaN)_n$ ($3 \leq n \leq 32$) clusters. It reveals that the larger the cluster, the greater the binding energy and hence a more stable structure and more stable photonic properties are expected.

To predict the photonic characteristics of the group III-N clusters, we need to use the TD-DFT approach to excite the ground state to the first excited state and then back to the ground state for light emission. Figure 3 shows the simulation process and the calculation procedures for the analysis of the absorption/emission spectra. Table 1 shows that there are bascially four steps: the first step is to perform the ground state optimization using the TI-DFT, which carries out the jobs of geometry optimization and frequency analysis; the second step is to analyze the absobtion process using the TD-DFT; the third step is for geometry optimization at the excited state; and the last step is to calculate the single point energy of the emission

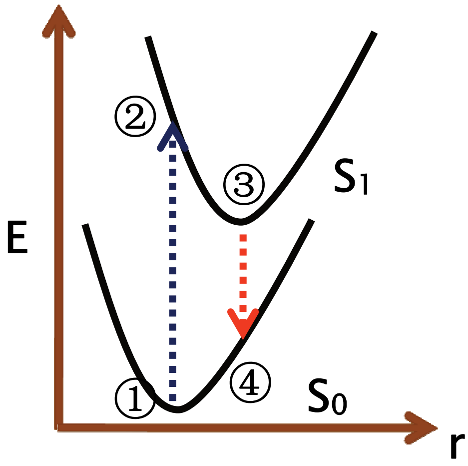

S_0: ground state

S_1: first excited state

Figure 3: Simulation steps to calculate the photonic properties during the absorption and the emission processes represented on an energy-versus-position diagram, where S_0 is the ground state and S_1 is the first excited state.

process. The last three steps all employ the TD-DFT, since they are time-dependent processes. Figure 4 shows the determination of the lowest unoccupied molecular orbital (LUMO) among the occupied orbitals, the highest occupied molecular orbital (HOMO) in the virtual orbitals, and the band gap between them on a density of states (DOS) diagram using the example of a $(GaN)_{26}$ cluster.

Figure 5 shows the optimized structures of the GaN clusters with variable sizes (more atoms and more rings). Their LUMOs and HOMOs are displyed on the energy level diagram. The figure reveals that the LUMOs and HOMOs are proportional to the size of the cluster, except the LUMO of the $(GaN)_5$, whose binding energy is too small to generate a stable cluster. Figure 6 shows the band gaps of all the $(GaN)_n$ clusters in our study. Four groups of different number (1-4) of rings can be categorized. They show different trend with the number (3-32) of the GaN units. When there are more rings the molecular structure becomes more stable and the quantum confinement effect makes the band gap increase with the reduction of the size of the clusters. Some of the exceptions might be due to the surface effect, since reducing the cluster size doesn't reducing the number of surface atoms proportionally. The surface atom effect can be explained by Fig. 7, which displays all the molecular orbitals of an example $(GaN)_{26}$ cluster. In which the green color

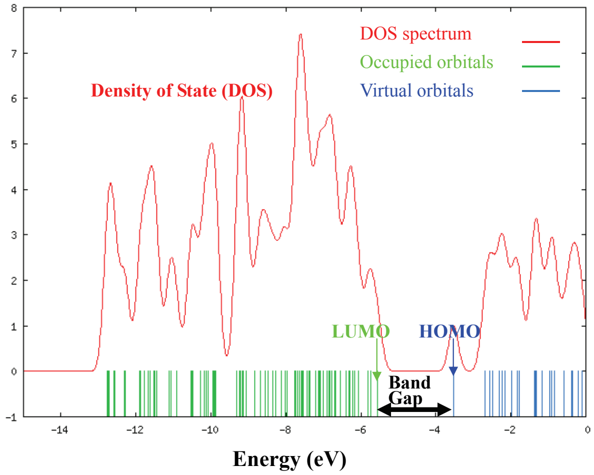

Figure 4: Determination of the lowest unoccupied molecular orbital (LUMO) in the occupied orbitals, the highest occupied molecular orbital (HOMO) in the virtual orbitals, and the band gap between them on the density of state (DOS) diagram of an example $(GaN)_{26}$ cluster.

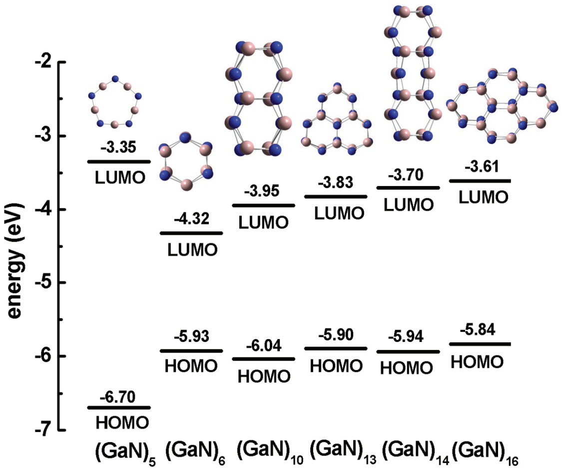

Figure 5: Optimized geometries and energy level positions of the LUMOs and HOMOs of GaN clusters with variable sizes (more atoms and more rings).

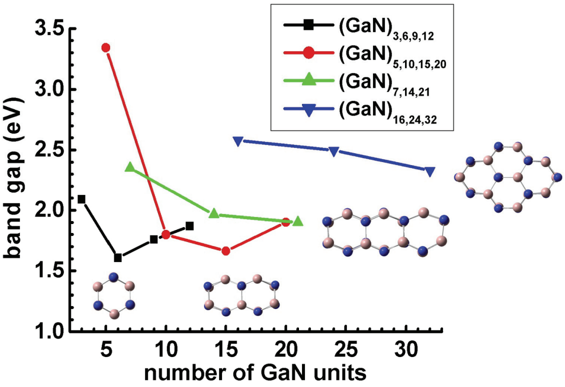

Figure 6: Band gaps of the $(GaN)_n$ clusters. Four groups of different number of rings show different trend with the number of the GaN units.

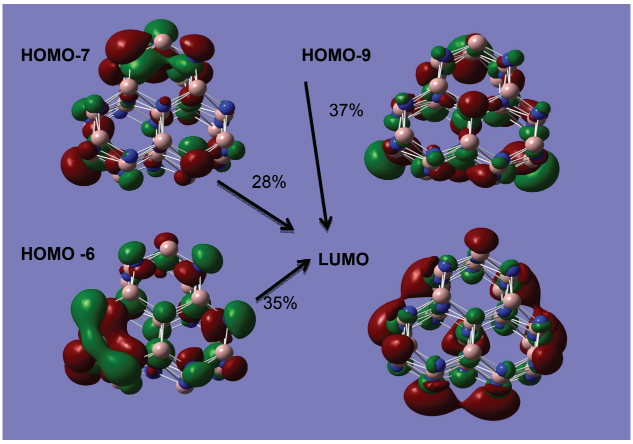

Figure 7: Molecular orbitals of the $(GaN)_{26}$. Green color indicates electrons spin up and brown color means spin down. Most electrons are distributed mainly on the surface atoms, instead of those bulk atoms. The electrons on the LUMO are mainly excited from the HOMO-9 (37%), the HOMO-7 (28%) and the HOMO-6 (35%).

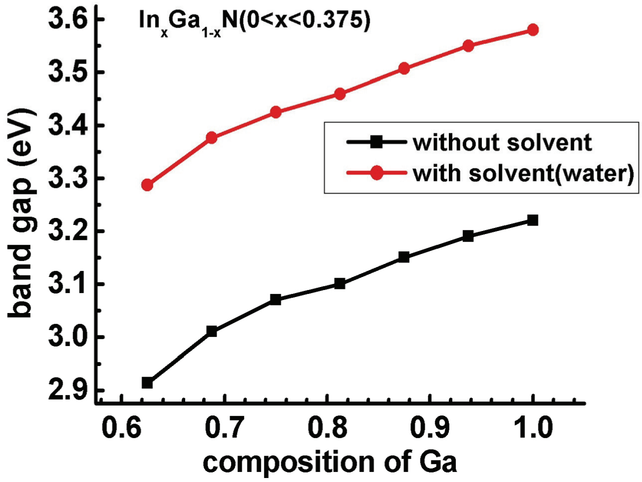

Figure 8: Band gaps of the ternary In$_x$Ga$_{1-x}$N clusters where $0 \leq x \leq 0.375$. The more the In atoms are doped in, the lower the band gap will be, with and without the solvent (water). The solvent effect is a blue shift in the spectrum, since the band gap becomes larger when the clusters are in the solvent.

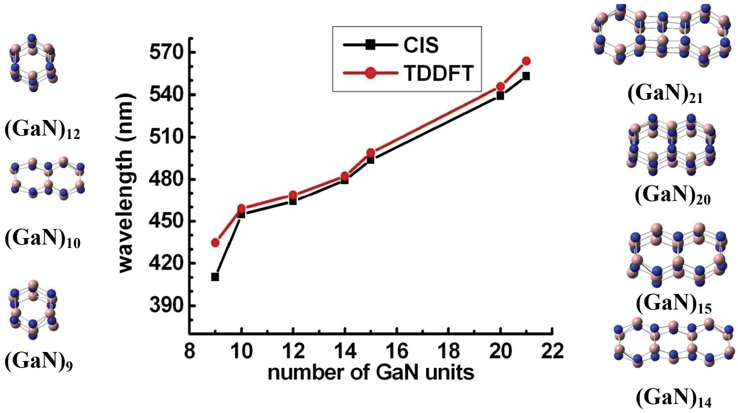

Figure 9: Peak wavelength calculations of the emission process of the binary (GaN)$_n$ using both CIS and TD-DFT methods. The number of GaN units varies from 9 to 21, and the wavelengths vary from 410 nm to 560 nm. That means the smaller the cluster the shorter the wavelength of the light emitted.

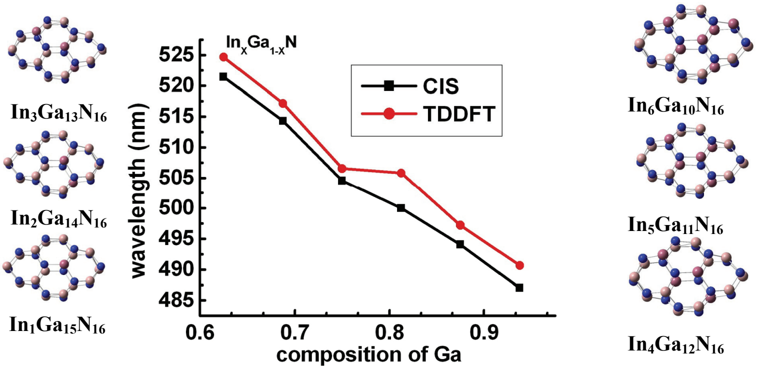

Figure 10: Peak wavelength calculations of the emission process of the ternary $In_xGa_{1-x}N$ using both CIS and TD-DFT methods. The composition of In varies from 0 to 0.375, and the wavelengths vary from 485 nm to 525 nm. That means the more the In atoms are doped the longer the wavelength of the light emitted.

indicates electrons spin up and the brown color means spin down. Most electrons are distributed mainly on the surface atoms, instead of those bulk atoms inside the $(GaN)_{26}$ cluster. The electrons on the LUMO are mainly excited from the HOMO-9 (37%), HOMO-7 (28%) and HOMO-6 (35%). The electrons distributed on the surface atoms dominate the photonic characteristics of the quantum-dot-like clusters. Hence, the quantum confinement effect doesn't increase regularly when the cluster size decreases.

It seems that reducing the binary GaN cluster dimension tends to increase the band gap and shift the emission color to a further blue region. This is not what the LED engineers want, instead we would like to decrease the band gap by doping indium (In) atoms into the binary cluster to become a ternary $In_xGa_{1-x}N$ cluster where $0 \leq x \leq 0.375$. This is shown in Fig. 8 which indicates that the more the In atoms are doped in, the lower the band gap will be, with and without the solvent (water). The solvent effect is a blue shift in the optical spectrum because the band gap becomes larger when the atom clusters are in the solvent. There are two methods to evaluate the photonic properties in the excited states, which equip with a more stable, higher energy electronic configuration of the molecular system. One is the TD-DFT as described in the previous section; the other one is called the configuration interaction singles (CIS) approach. Gaussian09 offers this CIS approach to model the excited states as combinations of single substitutions out of the Hatree-Fock ground state. Figure 9 displays the results from the peak wavelength calculations of the emission process of the binary $(GaN)_n$ using both CIS and TD-DFT methods. Both

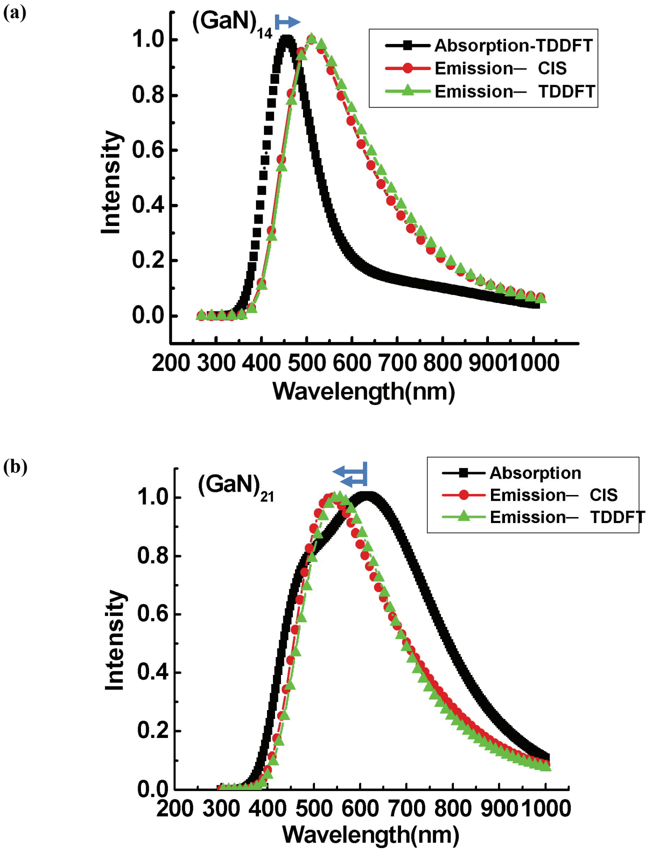

Figure 11: (a) Stokes shift takes place at $(GaN)_{14}$ between the absorption and the emission spectra; (b) anti-Stokes shift takes place at $(GaN)_{21}$.

approaches achieve the similar results with the same trend. The number of GaN units varies from 9 to 21, and the wavelengths change from 410 nm to 560 nm. That means the smaller the cluster the shorter the wavelength of the light emitted. Figure 10 shows the peak wavelength calculations of the emission process of the ternary $In_xGa_{1-x}N$ using both CIS and TD-DFT methods. The composition of In varies from 0 to 0.375, and the wavelengths vary from 485 nm to 525 nm. That means the more the In atoms are doped, the longer the wavelength of the light emitted. Figure 11 reveals that there is a wavelength shift between the locations of the band maxima in the absorption and in the emission spectra. This is due to the emitted photon has less (or more) energy than the absorbed photon, the energy difference is called Stokes (or anti-Stokes) shift. Figure 11 shows that a Stokes shift takes place at $(GaN)_{14}$ between the absorption and the emission spectra predicted; while an anti-Stokes shift takes place at $(GaN)_{21}$. That concludes the TD-DFT approach is necessary in modeling the LED photoluminescence characteristics. The predicted emission wavelength is different from the absorption wavelength calculated from the TI-DFT.

In order to estimate the size of those clusters, a sphere is assumed and the equivalent

Table 1: Simulations steps and the calculations performed for the analysis of the absorption and emission spectra

Simulation Step	**Job Type**	**Method**	**Basis Set**
1: ground state optimization	geometry optimization + frequency analysis	TI-DFT(B3LYP)	LanL2DZ
2: absorption	single point energy	TD-DFT(B3LYP)	LanL2DZ
3: excited state optimization	geometry optimization	TD-DFT(B3LYP)	LanL2DZ
4: emission	single point energy	TD-DFT(B3LYP)	LanL2DZ

Table 2: Molar volume and estimated equivalent diameter of the GaN clusters

$(GaN)_n$	molar volume (Bohr^3)	equivalent diameter (nm)
$(GaN)_6$	20055.022	1.78
$(GaN)_9$	23612.317	1.88
$(GaN)_{10}$	25542.657	1.93
$(GaN)_{12}$	27195.689	1.97
$(GaN)_{13}$	31941.675	2.08
$(GaN)_{14}$	28921.542	2.01
$(GaN)_{15}$	29496.459	2.03
$(GaN)_{16}$	37591.38	2.19
$(GaN)_{20}$	33603.855	2.12
$(GaN)_{21}$	35613.568	2.16
$(GaN)_{26}$	40766.545	2.26
$(GaN)_{32}$	47249.317	3.37

diameter is equated as:

$$d_c = 2(\frac{3V_m}{4\pi N})^{1/3} \tag{11}$$

where d_c is the equivalent cluster diameter, N is the Avogadro's number, V_m is the molar volume calculated by the Gaussian inside a contour with density of 0.001 electrons/Bohr^3. Table 2 indicates that the cluster diameter varies from 1.78 nm to 3.37 nm if the $(GaN)_n$ cluster varies from n=6 to n=32. It is not necessary that the size of the cluster becomes larger when n increases, because the molecular structure is configured ring by ring, layer by layer, not in radial expansion. That causes the band gap fluctuates when the dimension of the cluster becomes smaller and the surface atom effect of the clusters has to be taken into account.

4 Conclusion

Photonic characteristics of binary $(GaN)_n$ ($3 \leq n \leq 32$) clusters and ternary $In_xGa_{1-x}N$ ($0 \leq x \leq 0.375$) clusters have been studied in this paper, using the approach of the first-principles density functional theory. Quantum confinement due to the size effect has been proved. However, reducing the GaN cluster dimension can only increase the band gap, and the emission light tends to be further blue. This paper suggests that doping the indium atoms, also in the group III, into the GaN cluster may reduce the band gap. The color of the emission light can be controlled via both the indium concentration and the dimension of the cluster. This is important in the LED industry and further improvement in the photonic characteristics can be carried out through the modern nanotechnology.

Acknowledgement: Thanks are due to the National Science Council of Taiwan and the Tsing Hua Boost Program which supported this research under the grant numbers: NSC 98-2221-E-007-108-MY3 and NTHU99N2521E1. We are also grateful to the National Center for High-Performance Computing for the generous computer time and facilities.

References

Becke, A. D. (1988): Density-functional exchange-energy approximation with correct asymptotic behavior. *Phys. Rev. A,* vol. 38 (6), pp. 3098–3100.

Brena, B.; Ojama, L. (2008): Surface effects and quantum confinement in nanosized GaN clusters: theoretical predictions. *J. Phys. Chem. C*, vol. 112, pp.13516–13523.

Carter, D. J.; Puckeridge, M.; Delley, B. and Stampfl, C. (2009): Quantum confinement effects in gallium nitride nanostructures: *ab inito* investigations. *Nanotechnology*, vol. 20, 425401 (5pp).

Fitzgerald, G.; Goldbeck-Wood, G.; Kung, P.; Petersen, M.; Subramanian, L.; Wescott, J. (2008): Materials modeling from quantum mechanics to the mesoscale. *CMES: Computer Modeling in Engineering & Science*, vol. 24, no. 3, pp. 169-183.

Foresman, J. B.; Frisch, A. (1996): *Exploring Chemistry with Electronic Structure Methods*, 2^{nd} Edition, Gaussian, Inc., Pittsburgh, PA.

Frisch, M. J.; Trucks, G. W.; Schlegel, H. B.; Scuseria, G. E.; Robb, M. A.; Cheeseman, J. R.; Scalmani, G.; Barone, V.; Mennucci, B.; Petersson, G. A.; Nakatsuji, H.; Caricato, M.; Li, X.; Hratchian, H. P.; Izmaylov, A. F.; Bloino, J.; Zheng, G.; Sonnenberg, J. L.; Hada, M.; Ehara, M.; Toyota, K.; Fukuda, R.; Hasegawa, J.; Ishida, M.; Nakajima, T.; Honda, Y.; Kitao, O.; Nakai, H.; Vreven, T.; Montgomery, Jr., J. A.; Peralta, J. E.; Ogliaro, F.; Bearpark, M.; Heyd, J. J.; Brothers, E.; Kudin, K. N.; Staroverov, V. N.; Kobayashi, R.; Normand, J.; Raghavachari, K.; Rendell, A.; Burant, J. C.; Iyengar, S. S.; Tomasi, J.; Cossi, M.; Rega, N.; Millam, N. J.; Klene, M.; Knox, J. E.; Cross, J. B.; Bakken, V.; Adamo, C.; Jaramillo, J.; Gomperts, R.; Stratmann, R. E.; Yazyev, O.; Austin, A. J.; Cammi, R.; Pomelli, C.; Ochterski, J. W.; Martin, R. L.; Morokuma, K.; Zakrzewski, V. G.; Voth, G. A.; Salvador, P.; Dannenberg, J. J.; Dapprich, S.; Daniels, A. D.; Farkas, Ö.; Foresman, J. B.; Ortiz, J. V.; Cioslowski, J.; Fox, D. J. (2009): *Gaussian 09, Revision A.1*, Gaussian, Inc., Wallingford CT.

Kandalam, A. K.; Blanco, M. A.; Pandey, R. (2002): Theoretical study of Al_nN_n, Ga_nN_n and In_nN_n (n=4, 5, 6) clusters. *J. Phys. Chem. B*, vol. 106, pp. 1945-1953.

Kohn, W.; Sham, L. J. (1965): Self-consistent equations including exchange and correlation effects. *Phys. Rev.*, vol. 140 (4A), A1133-A1138.

Lee, C.; Yang, W.; Parr, R. G. (1988): Development of the Colle-Salvetti correlation-energy formula into a functional of the electron density. *Phys. Rev. B,* vol. 37, p. 785.

Madelung, O. (1964): *Physics of III-V Compounds*, Wiley, New York.

Marques, M.A.L.; Ullrich, C.A.; Nogueira, F.; Rubio, A.; Burke, K.; Gross, E.K.U. (2006): *Time-Dependent Density Functional Theory*, Springer-Verlag.

Mura, T.; Koya, T. (1992): *Variational Methods in Mechanics*, Oxford University Press, New York.

Nakamura, S.; Mukai, T.; Senoh, M. (1991): High-power GaN p-n junction blue-light emitting diodes. *Jpn. J. Appl. Phys.,* vol. 30, pp. 1998-2001.

Nakamura, S.; Mukai, T. (1992): High-quality InGaN films grown on GaN films junction blue-light emitting diodes. *Jpn. J. Appl. Phys.*, vol. 31, pp. 1457-1457.

Nakamura, S.; Mukai, T.; Senoh, M. (1994): Candela-class high-brightness InGaN/AlGaN double-heterostructure blue-light-emitting diodes. *Applied Physics Letters*, vol. 64, pp. 1687-1689.

Nakamura, S.; Senoh, M.; Iwasa, N.; Nagahama, S. (1995): High-brightness InGaN blue, green and yellow light-emitting diodes with quantum well structures. *Jpn. J. Appl. Phys.*, vol. 34, pp. 797-799.

Nakamura, S.; Senoh, M.; Nagahama, S. ; Iwasa, N.; Yamada, T.; Matsushita, T.; Kiyoku, H.; Sugimoto, Y.; Kozaki, T.; Umemoto, H.; Sano, M. (1998): Continuous-wave operation of InGaN/GaN/AlGaN-based laser diodes grownon GaN substrates. *Appl. Phys. Lett.*, vol. 72, 2014.

Nakamura, S.; Fasol, G.; Pearton, S. J. (2000): *The Blue Laser Diode: The Complete Story*. 2^{nd} Edition, Springer.

Runge, E.; Gross, E. K. U. (1984): Density-functional theory for time-dependent systems. *Phys. Rev. Lett*, vol. 52(12), pp. 997–1000.

Slater, J. C. (1951): A simplification of the Hartree-Fock method. *Physical Review*, vol. 81, no. 3, pp. 385-390.

Song, B.; Cao, P. (2004): Geometric and electronic structures of small GaN clusters. *Physics Letters A*, vol. 328, pp. 364–374.

Srivastava, D.; Atluri, S. N. (2002): Computational nanotechnology: a current perspective. *CMES: Computer Modeling in Engineering & Science*, vol. 3, no. 5, pp. 531-538.

Sze, S. M.; Ng, K. K. (2007): *Physics of Semiconductor Devices*, 3^{rd} Edition, Wiley-Interscience.

Vosko, S. H.; Wilk, L.; Nusair, M. (1980): Accurate spin-dependent electron liquid correlation energies for local spin density calculations: a critical analysis. *Can. J. Phys.* vol. 58, p. 1200.

Wu, H.; Zhang, F.; Xu, X.; Zhang, C.; Jiao, H. (2003): Geometric and energetic aspects of aluminum nitride cages. *J. Phys. Chem. A*, vol.107, pp. 204- 209.

Zheludev, N. (2007): The life and times of the LED- a 100-year history. *Nature Photonics*, vol. 1, pp. 189-194.

Zhao, J.; Wang, B.; Zhou, X.; Chen, X.; Lu, W. (2006): Structure and electronic properties of medium-sized Ga_nN_nclusters (n = 4–12). *Chemical Physics Letters*, vol. 422, pp. 170–173.